AUTOMATED CRATER DETECTION IN THE SURFACE OF MERCURY IN MDIS-NAC IMAGERY. M. Pedrosa[1], P. Pina[2], M. Machado[2], L. Bandeira[2] and E. A. Silva[1], [1]FCT, UNESP, Presidente Prudente, BRAZIL (miriammmp@hotmail.com, erivaldo@fct.unesp.br), [2]CERENA, Instituto Superior Técnico, University of Lisbon, PORTUGAL (ppina@tecnico.ulisboa.pt, marlene.machado@tecnico.ulisboa.pt, lpcbandeira@tecnico.ulisboa.pt).

Introduction: In the last decade, a consistent evolution on the automated detection of impact craters on remotely sensed imagery from planetary surfaces is being reported in the literature (a good and complete review can be consulted in [1]). This route, from the initial and less generic approaches to the more recent and robust ones, permits now detecting craters with smaller dimensions with much higher performances on a wider variety of surfaces. This activity has been mainly performed on the surfaces of Mars [2], the Moon [3] and Phobos [4], also giving important contributions to the construction of crater catalogues. On the contrary, the automated identification of the craters of Mercury has not been yet addressed. Moreover, the global catalogues available for this planet, manually built, contain impact structures with its largest diameters (D), namely D>10 km [5] and D>20 km [6], both built upon the flybys of Mariner 10 and MESSENGER. Thus, this a task that we initiate now on Mercury, presenting the preliminary performances achieved with a method of ours on a set of images captured by the MDIS-NAC (narrow angle camera) of MESSENGER.

Method: The detection method we are applying now is the same adaptive one that was inspired by two previous works [7][8] and sucessfully put together into a single processing sequence [9], which achieved relevant crater detection performances on Mars [10] and Phobos [4]. We briefly remind that it consists of sequentially finding regions of the image that are good crater candidates (in order to substantially reduce the amount of information to analyse), on extracting a set of image characteristics (named Haar-like features) describing these candidates and also of some non-candidate samples, which are then classified into crater or non-crater with the aid of a robust classifier, Adaboost or SVM-Support Vector Machine. Since normally both perform equally well, we have now opted for the SVM classifier due to its faster computational time.

Experimental results: The detections of craters were performed inside Raditladi, a peak-ring crater of about 263 km in diameter and centred at 27.05ºN, 119.05ºE. The coverage of this impact structure by MESSENGER MDIS NAC images accounts, at the present date, about 500 images but with only less than half of them with resolutions in the range 15-75 m/pixel. In particular, we used a total of 10 map projected images, that were sequentially captured along two distinct rows with a bit different surface aspects, one more rough (row A), the other more smooth (row B). The MDIS-NAC images used are the following (footprints in Figure 1):

Row A: EN0221023192M (A1), EN0221023197M (A2), EN0221023202M (A3), EN0221023207M (A4), EN0221023213M (A5).

Row B: EN0221066394M (B1), EN0221066399M (B2), EN0221066404M (B3), EN0221066409M (B4), EN0221066414M (B5).

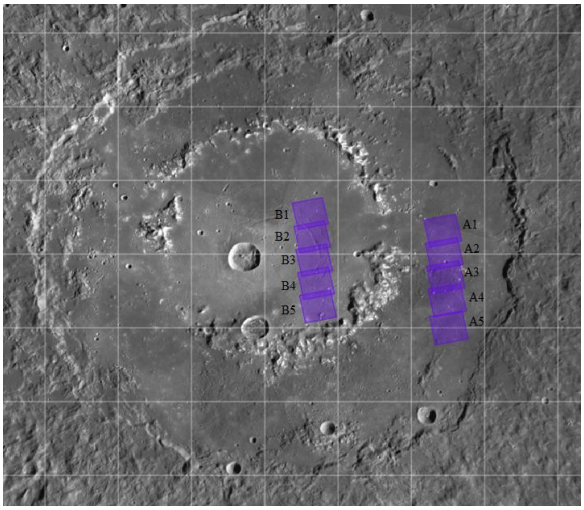

Figure 1. Raditladi crater and footprints of the 10 MDIS-NAC images used.

Our experimental strategy is to use information belonging to one single row to train the classifier and then test it with different images sets: only from the same row, only from the other row, and from both rows. This kind of cross-validation, typical in pattern recognition problems, permits us to better evaluate the robustness of the methodology but also to understand where and how higher efforts should be made in the training procedure to improve the performances. The quantities computed to evaluate the performances are the following:

1. Correct detections: D = 100 x TP/(TP + FN),
2. Quality: Q = 100 x TP/(TP + FP + FN)
3. Branching factor: B = FP/TP.

where, TP is the number of true positives (detected craters that are craters), FP is the number of false positives (detected craters that are not), and FN stands for the number of false negatives (non-detected craters).

Table 1. Automated detection performances.

Training image	Test images	TP (craters)	FP (craters)	FN (craters)	D (%)	Q (%)	B (index)
A1	A2-A5	1133	177	312	78.40	69.85	0.15
A1	B1-B5	1556	317	511	75.27	65.27	0.20
A1	A2-A5 + B1-B5	2689	494	823	76.57	67.12	0.18
B1	B2-B5	1318	539	391	77.12	58.63	0.40
B1	A1-A5	1591	499	345	82.18	65.34	0.31
B1	A1-A5 + B2-B5	2909	1038	736	79.65	61.98	0.35

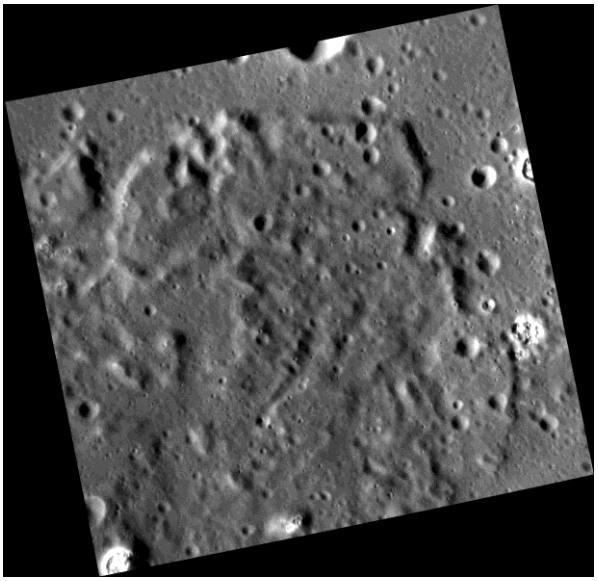

(a)

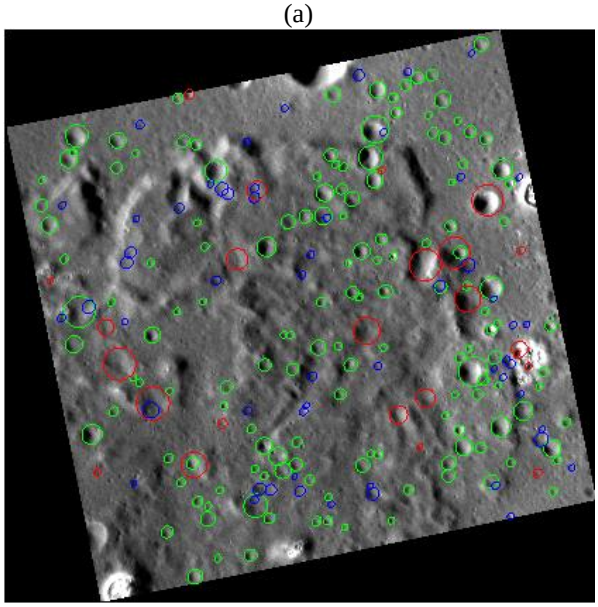

(b)

Figure 2. Automated detections: (a) Initial projected image MDIS-NAC EN0221023202M of about 17x17 km^2 with a spatial resolution of 16 m/pixel; (b) Circular shapes correspond to correct detections (green), false positives (red) and missing detections (blue).

The global detections obtained can be considered very good and similar in each experiment, with rates between 75 and 82% (an output example with the different results that can obtained is shown in Figure 2). On the contrary, the branching factor is more irregular, showing a good value when A1 was used for training (between 0.15 and 0.20), and doubling that value (0.31 to 0.40) when the image B1 was used in the training. This means that the selection of the samples for training set must be enhanced.

Conclusions and future work: These are preliminary results for Mercury, but already show the adequacy of our method to deal with automated detection of craters on that surface. Although the dataset used is relatively small (around 3000 craters), the surfaces analyzed are, from an image texture perspective, of moderate to difficult category. This permits us to face our future work on large detections on Mercury with some optimism.

References: [1] Salamuniccar G. and Loncaric S. (2012), *Horizons in Earth Science Research*, 8: 93-123, Nova Science. [2] Salamuniccar G. et al. (2011), *PSS*, 59: 111-131. [3] Salamuniccar G. et al. (2012), *PSS*,60: 236-247. [4] Salamuniccar G. et al. (2014), *ASR* (in press). [5] Herrick et al. (2011), *Icarus*, 215: 452-454. [6] Fassett et al. (2011), *GRL*, 38: L10202. [7] Martins et al. (2009) *IEEE GRSL*, 6: 127-131. [8] Urbach E. and Stepinski T. (2009), *PSS*, 57: 880-887. [9] Bandeira et al. (2012) *ASR*, 49: 64-74. [10] Bandeira et al. (2013), *AGU Fall Meeting*, ID 1796317.

Acknowledgments: This work was funded by the Portuguese Science Foundation (FCT) through project ANIMAR (PTDC/CTE-SPA/110909/2009) and support for MM and LB (SFRH/BPD/79546/2011).